Available online at www.sciencedirect.com
ScienceDirect
Catalysis Communications 8 (2007) 1934–1938
CATALYSIS COMMUNICATIONS
www.elsevier.com/locate/catcom

Hydrogen storage characteristics of metal oxide doped Al–MCM-41 mesoporous materials

Savidha Ramachandran, Jang-Hoon Ha, Do Kyung Kim *

Department of Material Science and Engineering, Korea Advanced Institute of Science and Technology (KAIST), Taejeon 305-701, Republic of Korea

Received 24 October 2005; received in revised form 15 March 2007; accepted 19 March 2007
Available online 4 April 2007

Abstract

The feasibility and perspectives of Al–MCM-41 as hydrogen storage systems were evaluated. The Al–MCM-41 with varying content of aluminum was synthesized by hydrothermal process. Different metal oxides were impregnated over Al–MCM-41 by incipient wetness impregnation (IWI) method. The crystallnity of the samples were interrogated by powder X-ray diffraction. The textural properties were measured by N_2 sorption method. The structural properties were established by Transmission Electron Microscope (TEM). The gas chromatogram indicates that hydrogen uptake in Al–MCM-41 is strongly dependent on density of Brønsted acid sites and the amount of metal oxide (especially NiO).

Keywords: Hydrogen; Storage; MCM-41; Nickel; Impregnation

1. Introduction

Hydrogen, for long has been proved to be the most ideal fuel for storage, transport and conversion of energy for a comprehensive clean energy concept [1]. Hydrogen as an energy carrier is limited by problems related to its storage. Concerning the point of hydrogen storage, as at room temperature and at atmospheric pressure hydrogen occupies about 3000 times the volume of gasoline providing the same amount of energy, it must be mechanically compressed, liquefied or subjected to some other sophisticated storage methods to be used for practical purpose [2–4]. Storage of hydrogen is either too expensive or too heavy, takes too much volume and/or is unsafe. Adsorptive storage of gaseous hydrogen is an inherently safe and attractive technology. Advanced materials under development to achieve this goal include metal hydrides, alloys, intermetallics, sodium and lithium alanates, nanotubes and carbon based materials [5]. Several metal hydrides are available commercially, representing a good solution for hydrogen storage. Among the various forms of carbon such as graphite, diamond, fullerenes and single walled carbon nanotubes, the carbon nanotubes were claimed to possess abnormal performance as a hydrogen carrier. However, there is a big controversy on this claim both experimentally and theoretically. The high storage capacity claimed already had not been reproducible by other researchers working in the same field [6].

The necessity for engineering a new type of hydrogen adsorbent arises since no approach satisfies all the factors viz, efficiency, size, weight, cost and safety requirements for personal transportation vehicles. More recently the interest in inorganic compositions and materials has shifted to the design of materials used in catalyst technology [7]. Porous crystalline solids build up from TO_4 tetrahedra, are potentially attractive materials for the safe storage of significant amounts of hydrogen [8]. The application of zeolites as a hydrogen storage system has only been discussed in a few publications among the various available TO_4 tetrahedra materials. Zeolites have been tried for its potential as a hydrogen storage system since they have a characteristic high internal surface area, approximately of a similar order of magnitude to the surface area of

* Corresponding author. Tel.: +82 42 869 4118; fax: +82 42 869 3310.
E-mail address: dkkim@kaist.ac.kr (D.K. Kim).

1566-7367/$ - see front matter © 2007 Elsevier B.V. All rights reserved.
doi:10.1016/j.catcom.2007.03.029

activated carbons, a material, which has appreciable hydrogen uptake values at cryogenic temperatures [9]. Previous studies have reported that zeolites can store small amount of hydrogen (0.3 wt%) if loaded at room temperature [10–12] or at temperatures >200 °C [11,12]. But, at cryogenic temperatures, substantially higher hydrogen storage capacities (>1 wt%) can be achieved. Adsorption in zeolite is a matter of pore filling and the usual surface area concepts are not applicable. The forces involved in this process are essentially physical (dispersive) and the enthalpies involved are low [13]. The primary focus has predominantly been on zeolites among the aluminosilicates, to date.

The objectives of this contribution are to present our preliminary promising catalytic results of the hydrogen adsorption capacity of mesoporous MCM-41 [14]. However, like zeolites these materials are not sufficiently light to represent the final solution of H_2 storage. However, they can also be ideal systems to investigate the interaction of H_2 with both dispersive and electrostatic forces [12]. The basic idea is to find an appropriate metal cation to modify MCM-41 and to find the relation between the cation and hydrogen storage property. Since, their transition metal substituted derivatives have been in focus of research as well and have created a renaissance of interest in the synthesis of porous materials [15]. Hitherto, the real effect of monometallic nickel on the level of hydrogen storage has not still received much attention [16]. Zielinski et al. reported the hydrogen storage capacity of nickel catalysts supported on amorphous activated carbon [17]. Mesoporous materials can accommodate nanoparticles of very high adsorption properties. This is the driving force in us to select mesoporous materials for hydrogen adsorption. The work presents the performance of various metal oxides such as TiO_2, Cr_2O_3, Fe_2O_3 and NiO doped Al–MCM-41 materials in the hydrogen storage capacity.

2. Experimental

The Al–MCM-41 (Si/Al = 25, 50, 100 and 200) was synthesized hydrothermally in a Teflon-lined stainless steel autoclave at 100 °C for 48 h, according to the procedure described earlier [18]. The typical gel composition was $2SiO_2$:$0.27(CTA)_2O$:$0.26Na_2O$:$0.26(TMA)_2O$:$0.017Al_2O_3$:$120H_2O$. The acid form of Al–MCM-41 was prepared from the Na form of Al–MCM-41 as per the procedure described earlier [18]. The Ni–Al–MCM-41 (25) was synthesized by adopting the same procedure using nickel nitrate as the source for nickel. The Al–MCM-41 was used as the host material to include various guest metal oxides. The metal oxides were impregnated by Incipient Wetness Impregnation (IWI) method using metal nitrate. The resulting (as-synthesized) Al–MCM-41, Ni–Al–MCM-41 and the impregnated materials were calcined at 550 °C in nitrogen for 1 h followed by air for 5 h. The materials were characterized by various physicochemical techniques. The crystallnity of samples were interrogated by powder X-ray diffractometer (D/max-IIIC, Rigaku, Tokyo, Japan). The textural properties were measured by N_2 sorption method. Structural characterization was analyzed by Transmission electron microscope (F-20 Tecnai, Philips).

The acidity of the Al–MCM-41 (25, 50, 100 and 200) samples was analysed by TPD–NH3 using TGA method. Adsorption of ammonia was carried out on each sample in a quartz tube packed with 1.0 g of the catalyst. Initial flushing was carried out with dry nitrogen for 3 h. Then the system was evacuated (1.5×10^{-5} Torr) at 550 °C for 5 h and cooled to room temperature. Ammonia adsorption was carried out by passing the ammonia vapours over the catalyst bed. After adsorption, the system was evacuated to remove the physisorbed ammonia and again ammonia was passed through the system. The adsorption and evacuation processes were repeated five times for saturation of adsorption. The extent of ammonia adsorbed over each catalyst was measured by TGA in a TA 3000 Mettler system. Nitrogen as purge gas was passed during desorption of ammonia. The TGA study was conducted at a heating rate of 10 °C/min up to 600 °C.

Hydrogen adsorption measurements were carried out over Al–MCM-41 and the metal oxides doped Al–MCM-41 materials. The adsorbents are mostly hydrophilic so, prior to adsorption measurements, water is completely removed by activation at 550 °C for 6 h. About 0.05 g of the catalyst was loaded in a stainless steel bomb and mounted in a closed refrigerator. After evacuating the vessel, the sample was brought in contact with a definite amount of hydrogen under a well regulated pressure for a calculated time period. Degassing was achieved at room temperature by purging argon. A high pressure in the order of 15 MPa forces the hydrogen to enter the cavities, and then a decrease in the temperature traps the hydrogen inside the framework. This mechanism of the TO_4 tetrahedral material enables hydrogen storage. Similarly, a temperature increase allows hydrogen release. The amount of hydrogen desorbed was measured using gas chromatography. Hydrogen adsorption values were expressed in terms of weight percent (wt%) hydrogen in materials.

3. Results and discussion

3.1. Characterization

The XRD patterns of the calcined Al–MCM-41 materials with Si/Al ratio 25, 50, 100 and 200 are presented in Fig. 1. The catalysts exhibit an intense peaks in the 2θ of 1.8–2.2° due to (100) reflection, and small peaks due to higher order (200) and (210) reflections indicating the formation of well ordered mesoporous materials [19]. The unit cell dimensions estimated from XRD data show an increase in cell volume with increasing aluminum content. The isotherms of nitrogen adsorption and desorption on the mesoporous Al–MCM-41 (25) is shown in Fig. 2. It presents a type IV isotherm according to the classification of Brunauer et al. [20]. The isotherm displays a typical step at

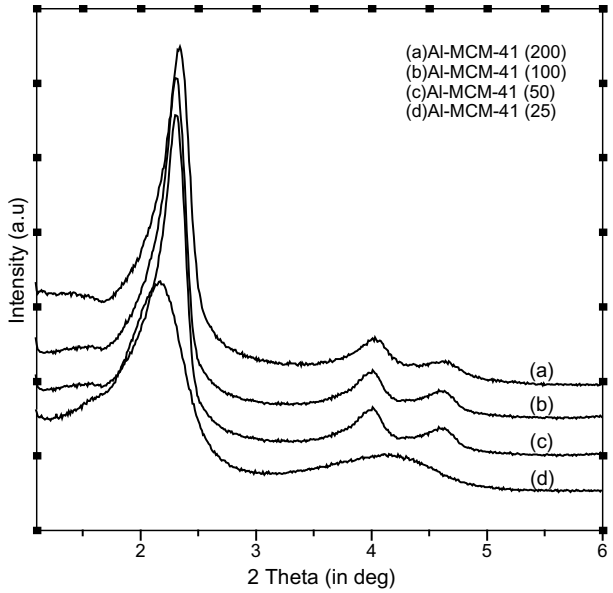

Fig. 1. CuKα X-ray diffraction patterns for Al–MCM-41 with different aluminium content.

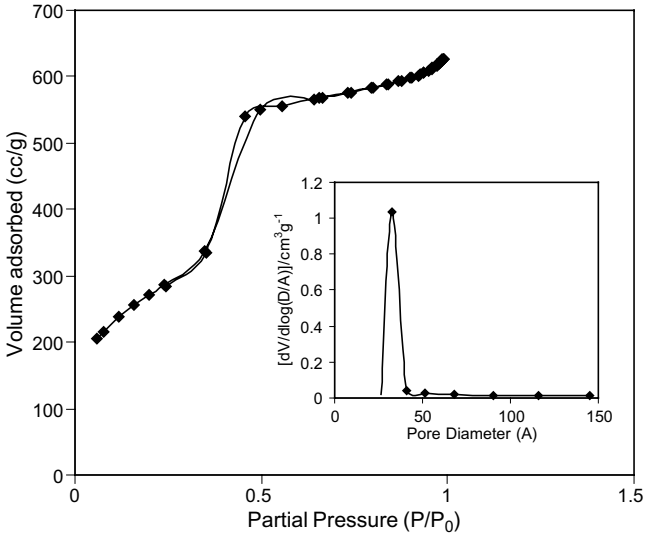

Fig. 2. A typical type IV nitrogen adsorption–desorption isotherms of Al–MCM-41 (25). The BJH pore size distribution is shown in the inset.

$P/P_0 \sim 0.4$ characteristic of capillary condensation within narrow mesopores of the MCM-41 structure. The textural properties of the Al–MCM-41 materials with varying Si/Al ratio are presented in Table 1. Calculation using BJH method show that the Al–MCM-41 sample has a narrow pore size distribution and the results are in good agreement with the previous report [21]. There is no significant change in the surface area, pore diameter and pore volume due to the impregnation of nickel (low level of loading). Fig. 3a and b show high-resolution electron microscopy (HREM) images of the calcined Al–MCM-41 (25) sample. Fig. 3a shows a uniform hexagonal arrangement of bright dots corresponding to the straight channels of Al–MCM-41.

Table 1
Textural properties of the calcined Al–MCM-41 catalysts determined from N_2 sorption studies

Catalysts	BET-surface area (m^2/g)	Pore diameter (Å)	Pore volume (cm^3/g)	Acidity (mmol/g)
Al–MCM-41 (200)	1360	50.0	1.45	0.13
Al–MCM-41 (100)	1159	45.9	1.17	0.21
Al–MCM-41 (50)	1025	42.0	1.07	0.27
Al–MCM-41 (25)	986	39.1	0.96	0.36

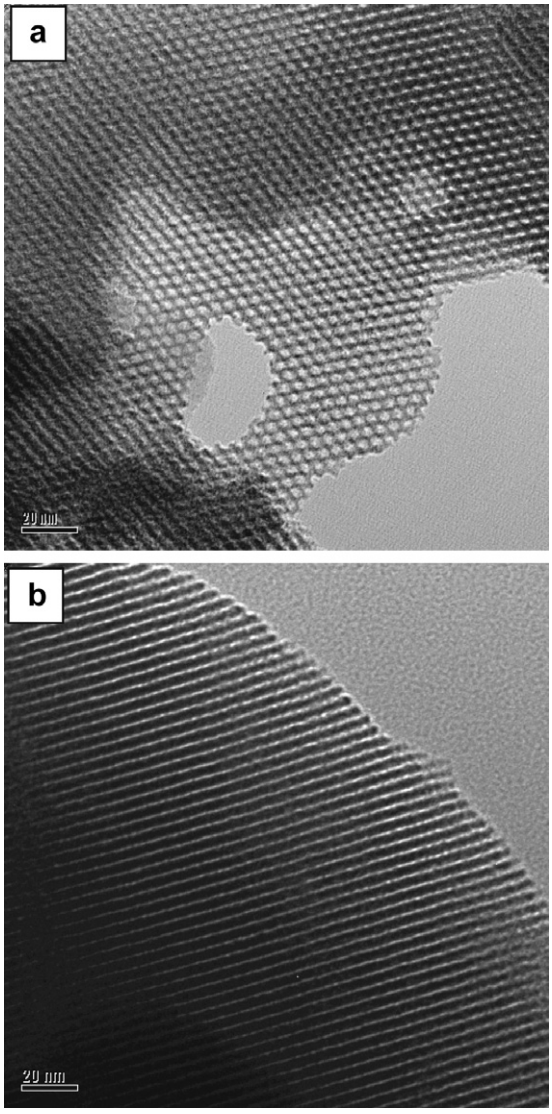

Fig. 3. Typical TEM micrograph of Al–MCM-41 (25) molecular sieves (a) hexagonal arrangement of pores and (b) Straight channels.

The brightness and the shape of the channels seem to differ slightly from place to place. This is a result of slight change in diffraction conditions. Fig. 3b shows the uniform channels from which the pore diameter can be calculated more

appropriately. The TEM micrographs for the Al–MCM-41 and their nickel impregnated samples confirm that the matrix structure is not modified after nickel impregnation (image not shown) [22]. The presence of both Brønsted and Lewis acid sites in Al–MCM-41 was confirmed from pyridine adsorbed FTIR study and the density of acid sites are calculated from the TPD–NH_3 and is presented in Table 1. It can be clearly seen from the data that the density of acid sites increases by increasing the amount of aluminum in the material.

3.2. Hydrogen adsorption

Hydrogen storage of the catalysts is dramatically increases with increasing specific surface area and pore volume as per the previous literature [17]. An increase in surface area can improve the H_2 adsorption properties because of the lack of specific interacting sites in the case of carbon nanotubes (CNT) and metal organic framework (MOF) [3]. But, in the case of molecular sieves, a possible link between the pore volume and hydrogen adsorption property is observed [9]. Hydrogen adsorption measurements of the Al–MCM-41 molecular sieves are presented in Fig. 4. It can be clearly seen that there is a significant change in hydrogen adsorption, though there is no considerable change in the pore volume (since metal oxide is present in subtle amount) due to the impregnation of metal oxides, which is in close agreement with Regli et al., reported that besides a high surface area, a peculiar framework topology combined with the presence of highly dispersed exposed polarizing species is relevant to increase the value of H_2 uptake [23].

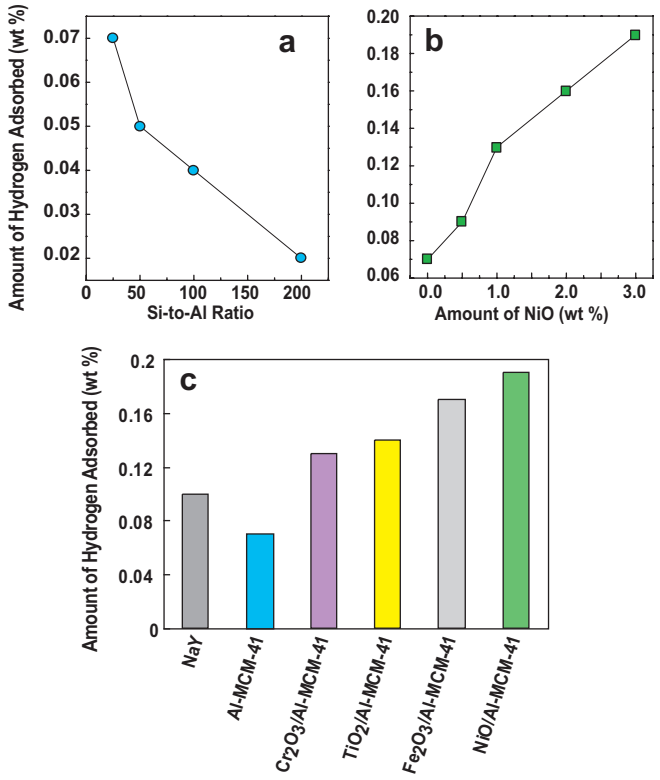

Fig. 4. Amount of hydrogen adsorbed in Al–MCM-41 (a) with different Si–Al ratio, (b) amount of hydrogen adsorbed in NiO-impregnated Al–MCM-41 (25) as a function of NiO content. (c) Hydrogen adsorption characteristics of various metal oxides impregnated over Al–MCM-41 (25) mesoporous materials, compared with commercial NaY zeolite.

The amount of hydrogen adsorbed with respect to aluminum content in Al–MCM-41 (25, 50, 100 and 200) is correlated in Fig. 4a. From the graph it can be depicted that the amount of hydrogen adsorbed is proportional to the aluminum content, which could be due to the increment in the protonic sites (Brønsted acid sites). From Table 1 it can be clearly seen that the amount of hydrogen adsorbed is not proportional to the surface area as in the case of CNT. This sorption is sufficient to distort the electronic cloud of hydrogen; as a result the center of symmetry of hydrogen is destroyed. Hence, there is a change from higher symmetry D_{2h} point group to lower symmetry C_{2v} point group. The Brønsted acidity plays a major role in adsorption capacity, hence, the divalent nickel is an interesting substitutent for aluminum in Al–MCM-41, since its presence in the lattice position (with tetrahedral coordination) can provide double negative charges, and a consequent increase in the number of Brønsted acid sites. Comparison of the storage capacity of Ni–MCM-41 with Al–MCM-41 exhibits that the former is observed to be more capable (0.13 wt%) than the later (0.07 wt%), which could be due to the more Brønsted acid sites planted by the Ni^{2+} ion.

Researchers have reported that higher uptake can be achieved due to cationic vibrations at higher temperatures making the cages more accessible in the ion-exchanged materials [24]. In the current project, we analyze the hydrogen adsorption capacity of the metal oxides such as Cr_2O_3, TiO_2, Fe_2O_3 and NiO (3 wt%) doped Al–MCM-41 (25), since metals differ in the ability to dissociate hydrogen. But, due to the confined size of the nanomaterials, the stabilization is difficult in the absence of mesopores, they may readily agglomerate to form bulk particles. Hence, MCM-41 acts as a better support for metal oxide catalysts. The hydrogen dissociation ability of the metals depends on surface structure, morphology and purity and is independent of surface area of the metal doped Al–MCM-41 which is found to be 986.7, 952.3, 973.2, 856.3 and 813.3 m^2/g for Al–MCM-41 (25), Cr_2O_3, TiO_2, Fe_2O_3 and NiO doped Al–MCM-41 (25), respectively. Fig. 4c presents the effect of various metal oxide nanoclusters impregnated on Al–MCM-41 (25). The graph clearly depicts that there is a significant increment in the hydrogen storage capacity by metal oxide doping, which could be due to the quite high adsorption properties due to high surface free energy of the nanodimension particles. In addition, the excess uptake due to metal oxide impregnation could be attributed to hydrogen adsorption process through a spillover mechanism namely the dissociation of hydrogen on the metal phase and subsequent migration onto the support.

Both Cr_2O_3 and TiO_2 doped Al–MCM-41 exhibits almost same storage capacity. A subtle increase in the hydrogen adsorption capacity of TiO_2 doped Al–MCM-41 may be due to the semi conducting property of titania. Fe_2O_3 shows intermediate adsorption capacity between TiO_2 and NiO doped Al–MCM-41, which could be due to the presence of iron in higher oxidation state. Among the various metal oxides doped Al–MCM-41 studied, NiO/Al–MCM-41 (25) shows better adsorption, which could be due to the dehydrogenating property of nickel. In addition, framework Ni–O bond can also involve in hydrogen adsorption. Zielinski et al., reported that nickel catalysts supported on amorphous activated carbon could significantly improve the hydrogen storage at room temperature as compared to the support [17]. It is not yet clear whether the observed differences in adsorption values are due to pore blocking by metal oxides, or variations in the interaction of hydrogen with different cations. Since, the amount of hydrogen adsorbed is proportional to the amount of nickel oxide, we allocated the amount adsorbed to NiO to construct in the Fig. 4b. After the NiO impregnation the surface area, pore diameter and pore volume remains almost the same, due to low level of loading. The surface area is found to be 906, 856, 823 and 813 m^2/g for 0.5, 1, 2 and 3 wt% NiO doped Al–MCM-41 (25). Hence, the increment in the adsorption capacity may be due to the ability of the metal surface to dissociate the hydrogen molecule, and the consequent migration of the atoms to the substrate (spillover mechanism). The adsorption capacity of reduced metal oxide on Al–MCM-41 substrate is under investigation. The hydrogen adsorption mechanism is still a mater of debate. Further work is required to understand fully these mechanisms.

4. Conclusion

The storage of hydrogen over Al–MCM-41 and various metal oxides doped Al–MCM-41 (25) has been demonstrated successfully. The study shows that the hydrogen adsorption depends on the metal cation, attributed to the difference in the density of Brønsted acid sites. NiO impregnation on Al–MCM-41 enhances the storage of hydrogen to significant amounts. The hydrogen spillover is mainly responsible for the enhanced hydrogen adsorption by increasing the NiO content. The studies indicate the potential of mesopores as good candidates to form and stabilize nanomaterials within their pores. They can also be better exploited for better adsorption properties even by producing mono-, bi-, and tri-metal alloys for hydrogen storage properties and this supports can excel all the others.

Acknowledgement

Financial support from the Center for Advanced Materials Processing (CAMP) of the 21st Century Frontier R&D Program funded by the Korean Ministry of Science and Technology and Brain Korea 21 Program from Korean Ministry of Education are gratefully acknowledged.

References

[1] A.M. Seayad, D.M. Antonelli, Adv. Mater. 16 (2004) 765.
[2] A. Zuttel, Naturwissenschaften 91 (2004) 157.
[3] L. Schlapbach, A. Zuttel, Nature 414 (2001) 353.
[4] G.D. Berry, S.M. Aceves, Energy Fuels 12 (1998) 49.
[5] J.K. Borchardt, Mater. Today 7 (2004) 30.
[6] L. Zhou, Y. Zhou, Y. Sun, Int. J. Hydrogen Energy 29 (2004) 319.
[7] A.W.C. Van den Berg, S.T. Bromley, E. Flikkema, J. Wojdel, Th. Maschmeyer, J.C. Jansen, J. Chem. Phys. 120 (2004) 10285.
[8] A.W.C. Van den Berg, S.T. Bromley, J.C. Jansen, Micropor. Mesopor. Mater. 78 (2005) 63.
[9] M.G. Nijkamp, J.E.M.J. Raaymakers, A.J. Van Dillen, K.P. de Jong, Appl. Phys. A 72 (2001) 619.
[10] S.B. Kayiran, F.L. Darkrim, Surf. Interf. Anal. 34 (2002) 100.
[11] H.W. Langmi, A. Walton, M.M. Al-Mamouri, S.R. Johnson, D. Book, J.D. Speight, P.P. Edwards, I. Gameson, P.A. Anderson, I.R. Harris, J. Alloys Compd. 356–357 (2003) 710.
[12] J. Weitkamp, M. Fritz, S. Ernst, Int. J. Hydrogen Energy 20 (1995) 967.
[13] C.H. Wu, J. Chem. Phys. 71 (1979) 783.
[14] J.S. Beck, J.C. Vartuli, W.J. Roth, M.E. Leonowicz, C.T. Kresge, K.D. Schmitt, C.T-W. Chu, D.H. Olson, E.W. Sheppard, S.B. McCullen, J.B. Higgins, J.L. Schlenker, J. Am. Chem. Soc. 114 (1992) 10834.
[15] A. Tuel, Micropor. Mesopor. Mater. 27 (1999) 151.
[16] A. Lueking, R.T. Yang, AIChE J. 49 (2003) 1556.
[17] M. Zielinski, R. Wojcieszak, S. Monteverdi, M. Mercy, M.M. Bettahar, Catal. Commun. 6 (2005) 777.
[18] R.B. Borade, A. Clearfield, Catal. Lett. 31 (1995) 267.
[19] C.T. Kresge, M.E. Leonowicz, W.J. Roth, J.C. Vartuli, J.S. Beck, Nature 359 (1992) 710.
[20] S. Brunauer, L.S. Deming, W.E. Deming, E. Teller, J. Am. Chem. Soc. 62 (1940) 1723.
[21] Z. Luan, C.F. Cheng, W. Zhou, J. Klinowski, J. Phys. Chem. 99 (1995) 1018.
[22] R. Wojcieszak, S. Monteverdi, M. Mercy, I. Nowak, M. Ziolek, M.M. Bettahar, Appl. Catal. A. Gen. 268 (2004) 241.
[23] L. Regli, A. Zecchina, J.G. Vitillo, D. Cocina, G. Spoto, C. Lamberti, K.P. Lillerud, U. Olsbye, S. Bordiga, Phys. Chem. Chem. Phys. 7 (2005) 3197.
[24] V.V. Krishnan, S.L. Suib, D.R. Corbin, S. Schwarz, G.E. Jones, Catal. Today 31 (1996) 199.